

Subsystem symmetries, quantum cellular automata, and computational phases of quantum matter

David T. Stephen,¹ Hendrik Poulsen Nautrup,² Juan Bermejo-Vega,³ Jens Eisert,³ and Robert Raussendorf⁴

¹Max-Planck-Institut für Quantenoptik, Hans-Kopfermann-Straße 1, 85748 Garching, Germany

²Institut für Theoretische Physik, Universität Innsbruck, Technikerstr. 21a, A-6020 Innsbruck, Austria

³Dahlem Center for Complex Quantum Systems, Freie Universität Berlin, 14195 Berlin, Germany

⁴Department of Physics and Astronomy, University of British Columbia, Vancouver, British Columbia V6T 1Z1, Canada

(Dated: December 14, 2024)

Recent years have seen significant progress in capturing and classifying phases of matter within the framework of tensor networks. In this work, we study symmetry protected topological (SPT) phases protected by subsystem symmetries. Building upon the general framework laid out, we demonstrate how they can be used in notions of measurement-based quantum computing. We define subsystem symmetries via quantum cellular automata (QCA) and use tensor networks to show that non-trivial SPT order under these symmetries is characterized by the presence of the QCA on the virtual level of the tensor network. This provides a possible avenue to classify SPT phases protected by subsystem symmetries. We then show that all QCA defining diagonal line-like or fractal symmetries can be used to construct new computationally universal phases of matter, in which every state is a resource for universal measurement-based quantum computation.

Symmetries are an essential tool for identifying and classifying quantum phases of matter. Even in the absence of both symmetry breaking and intrinsic topological order, gapped quantum systems at zero temperature can form distinct phases, which are the so called *symmetry-protected topological (SPT) phases* [1–6]. From familiar symmetries such as time-reversal symmetry or global spin-rotation symmetry, one can construct well-known SPT phases such as topological insulators [5, 7] and the Haldane phase [8, 9]. Other symmetries such as crystalline symmetries can also define distinct SPT phases [10–12]. It has become one of the notable endeavors in theoretical condensed matter physics to understand and classify those phases of matter.

Recently, another class of symmetries has emerged in several contexts in both the condensed matter and quantum information communities. These are symmetries which act non-trivially only on lower-dimensional subsystems of the whole system. These include “higher-form” symmetries which are related to higher-form gauge theories [13, 14] and have recently appeared in the construction of quantum memories and quantum error correction [15–18]. More relevant to the present work are the symmetries which act on rigid lower-dimensional lines or planes [14, 19, 20], or even fractals of non-integer dimension [16, 21, 22]. These *subsystem symmetries* have recently been shown to be closely related to fracton order [14, 16, 20, 21].

Questions of the classification of phases are primarily of concern for condensed matter physics. However, they are increasingly also the subject of study in quantum information theory, a field of research that is becoming increasingly intertwined with the former. In particular, phases of matter play a role in the framework of *measurement-based quantum computation (MBQC)*, a scheme of quantum computing that is performed only by local measurements on initial entangled states. Indeed, in recent work [23], a computationally universal phase of quantum matter was constructed. Within this phase, every ground state is a resource for universal MBQC [24, 25]. The phase of matter under consideration, the “cluster phase”, is an example of a two-dimensional subsystem symmetry-protected

topological phase which is protected by rigid one-dimensional line-like symmetries. This link between quantum phases and quantum computation was suggested some years ago and has since then been increasingly substantiated [26–41].

Indeed, recent years have seen the development of a close to complete link between one-dimensional SPT phases and MBQC [26–35]. In two spatial dimensions, this link is less developed to date, but progress has been made [36–41], with the cluster phase being the first universal computational phase of matter. There is an analogous link existing for topologically ordered systems in two-dimensions, whose anyonic excitations can be levied to achieve for error-resilient topological quantum computation [42–44]. In both cases, the same framework that is used to classify the phases of matter can also be used to understand their computational capability.

In this work, we use tensor networks to gain a deeper understanding of SPT phases protected by *subsystem symmetries* in general from a condensed matter perspective, as well as concerning their computational capability, taking a perspective of quantum information. We establish a strong link between subsystem symmetries and *quantum cellular automata (QCA)* by using QCA to define both rigid *line-like* and *fractal symmetries*. We show that, for all states with non-trivial SPT order under such a symmetry, the same QCA that defines the symmetry also appears on the virtual level of the tensor network. This means the patterns of entanglement found in these phases are characterized in part by QCA, demonstrating the possible use of tensor networks in obtaining a classification of SPT order under subsystem symmetries.

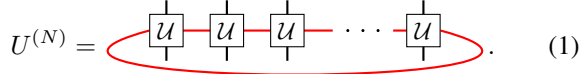
We then turn to investigating the computational capability of the constructed phases and show that, for all QCA that lead to diagonal line-like or fractal symmetries, we can define SPT phases that are computationally universal in the same way as the cluster phase. The computational schemes we develop are strictly tied to the QCA that define the phases, further strengthening the connection between quantum computation and SPT phases of matter in two dimensions.

In Sec. I, we begin with a review the basic properties of QCA. In Sec. II, we use QCA to define PEPS and show that

they have non-trivial SPT order under certain subsystem symmetries. Then, in Sec. III, we investigate the properties of the corresponding SPT phases in a quasi-1D picture before moving to a genuine 2D picture in Sec. IV. Finally, in Sec. V, we classify these phases by their computational power in measurement-based quantum computing.

I. Quantum cellular automata

In this section, we present a review of *quantum cellular automata* (QCA) for qubit systems, as described in Refs. [45–47], as they will become important in our description of symmetry protected topological order with respect to subsystem symmetries. A 1D QCA is a translationally-invariant locality-preserving unitary on a 1D chain of qubits [45]. That is, a QCA maps any locally supported operator to another locally supported operator, with the size of the support increased by a constant amount, independent of the size of the original support. In Ref. [48], it was shown that QCA acting on 1D systems are equivalent to *matrix product unitaries* (MPU), in that every QCA can be represented as an MPU with finite bond dimension, and every MPU is a QCA. An MPU is a matrix product operator defined by a local tensor \mathcal{U} , which generates a unitary $U^{(N)}$ on a ring of arbitrary length N . Graphically, the MPU can be represented by the tensor network



$$U^{(N)} = \text{---} \left(\begin{array}{c} | \\ \text{---} \text{U} \text{---} \\ | \end{array} \right) \text{---} \left(\begin{array}{c} | \\ \text{---} \text{U} \text{---} \\ | \end{array} \right) \text{---} \left(\begin{array}{c} | \\ \text{---} \text{U} \text{---} \\ | \end{array} \right) \text{---} \cdots \text{---} \left(\begin{array}{c} | \\ \text{---} \text{U} \text{---} \\ | \end{array} \right) \text{---} \quad (1)$$

Here, the colored lines represent the virtual indices of the MPU. All QCA described in this paper act on systems with periodic boundary conditions. Note that we use the graphical language of tensor networks extensively throughout this work (see Ref. [49] for a review of the relevant notation and concepts).

In what follows, we will focus on *Clifford quantum cellular automata* (CQCA) [46, 47], which are QCA that map products of Pauli operators to products of Pauli operators. For reasons of simplicity of notation, we focus on the Pauli Clifford group for qubits, even though the formalism laid out here could be applied larger dimensions as well [50, 51]. More precisely, on a finite system of N qubits, we can define the Pauli group \mathcal{P}_N as the group generated by all local Pauli operators X_i , Y_i , and Z_i acting on qubit i , where i is defined modulo N and can take negative values giving, for example, $X_{-1} = X_{N-1}$. The Pauli group forms a faithful irreducible projective representation of $\mathbb{Z}_2^N \times \mathbb{Z}_2^N$. A CQCA is a QCA that is also an automorphism of \mathcal{P}_N , defined by a transition function T such that $P \mapsto T(P)$ for any $P \in \mathcal{P}_N$.

CQCA have been studied extensively in Refs. [46, 47] which introduced a compact representation of CQCA. Firstly, a CQCA T is completely specified by the images $T(X_0)$ and $T(Z_0)$. To see this, note that a) the QCA is translationally invariant, b) X_i and Z_i generate the whole Pauli group up to phases, which contains a basis of the space of

all $2^N \times 2^N$ matrices. Next, we represent the group $\mathbb{Z}_2^N \times \mathbb{Z}_2^N$ (and therefore \mathcal{P}_N , up to phases) by $2N$ -component binary strings $\xi = (\xi^X, \xi^Z)$ such that

$$P(\xi) = \bigotimes_{i=1}^N X_i^{\xi_i^X} Z_i^{\xi_i^Z} \in \mathcal{P}_N. \quad (2)$$

We further condense the notation using the language of Laurent polynomials [46]. We map ξ onto a vector of polynomials of a variable u as

$$\begin{pmatrix} \xi^X \\ \xi^Z \end{pmatrix} \mapsto \begin{pmatrix} \sum_i (u^i)^{\xi_i^X} \\ \sum_i (u^i)^{\xi_i^Z} \end{pmatrix}.$$

The purpose of the variable u is to keep track of the moving and spreading of local Pauli operators under T . For example, the operator $X_1 Z_0 X_{-1}$ is represented as

$$\begin{pmatrix} u + u^{-1} \\ 1 \end{pmatrix}. \quad (3)$$

We use the symbol ξ to represent both the binary and polynomial representations of an element of \mathcal{P}_N interchangeably. Finally, we can represent the CQCA T as a 2×2 matrix t of polynomials by arranging

$$T(X_0) := t \begin{pmatrix} 1 \\ 0 \end{pmatrix}, \quad T(Z_0) := t \begin{pmatrix} 0 \\ 1 \end{pmatrix} \quad (4)$$

into columns of a matrix. For a concrete example, consider the CQCA T_g defined by the relations

$$T_g(X_i) = X_{i-1} Z_i X_{i+1}, \quad T_g(Z_i) = X_i. \quad (5)$$

This CQCA is the QCA of the 2D cluster state [25], and it has appeared several times already in the context of quantum computation [52–54]. In the polynomial representation, this CQCA becomes

$$t_g = \begin{pmatrix} u + u^{-1} & 1 \\ 1 & 0 \end{pmatrix}.$$

Every CQCA T can be represented as a 2×2 matrix t whose entries are Laurent polynomials over \mathbb{Z}_2 , up to phase factors [46]. We further restrict to those matrices which have unit determinant. This corresponds to the scenario where the images $T(X_i)$, $T(Z_i)$ are symmetric about site i , meaning there is no translation in the CQCA [46] [55]. We make this restriction only because translation will not be particularly interesting for our purposes. With this restriction, we have that all entries in t are symmetric Laurent polynomials, meaning that u^{-k} appears whenever u^k does, for all k [46].

CQCA can be split into three classes depending on their trace [47].

- *Periodic CQCA*. When $\text{Tr}(t) = 0$ or 1 the CQCA has *periodic* behavior.

- *Glider CQCA*. When $\text{Tr}(t) = u^c + u^{-c}$ for some positive integer c , the CQCA supports *gliders*. These are operators on which the CQCA acts as translation by $\pm c$ sites.
- *Fractal CQCA*. If neither of these conditions hold, the CQCA will display self-similar *fractal* behavior.

The CQCA in Eq. (5) supports gliders, with $\text{Tr}(t_g) = u + u^{-1}$. Indeed, we can check that $T_g(X_i Z_{i-1}) = X_{i+1} Z_i$, and $T_g(Z_{i+1} X_i) = Z_i X_{i-1}$.

The Laurent polynomial representation allows us to uncover an identity which will be useful at several points throughout this work. Namely, due to the Cayley-Hamilton theorem, we obtain [47]

$$t^2 = \text{Tr}(t)t + \mathbb{I}, \quad (6)$$

where we have used our assumption that $\det(t) = 1$, and the fact that the polynomials are defined over the field \mathbb{Z}_2 , so addition and subtraction are equivalent. This useful equation allows us to reduce powers of t to linear combinations of t and \mathbb{I} .

II. Defining PEPS from QCA

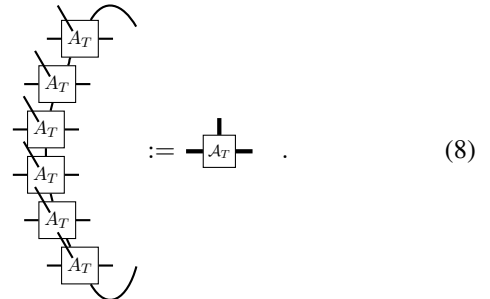
Now we use the correspondence between QCA and MPU to define *projected entangled pair states (PEPS)* [56]. Given a CQCA T , we first represent it as an MPU with local tensor \mathcal{T} , using the technique of Ref. [48]. We then define the PEPS in terms of \mathcal{T} by a local tensor \mathcal{A}_T whose components are given by

$$\begin{array}{c} |+\rangle \\ \downarrow \\ \square_{\mathcal{A}_T} \end{array} := \begin{array}{c} \text{---} \\ | \\ \text{---} \\ \square_{\mathcal{T}} \\ \text{---} \\ | \\ \text{---} \end{array}, \quad \begin{array}{c} |-\rangle \\ \downarrow \\ \square_{\mathcal{A}_T} \end{array} := \begin{array}{c} \text{---} \\ \circ \\ \text{---} \\ \square_{\mathcal{T}} \\ \text{---} \\ | \\ \text{---} \end{array}. \quad (7)$$

From a given \mathcal{T} the PEPS tensors for local qubit dimension can be uniquely defined in this way, the vectors $\{| \pm \rangle\}$ constituting a basis. The resulting PEPS may not be rotationally invariant; the bond dimension along the horizontal and vertical directions may not even match. Since we will be mainly treating these PEPS as quasi-1D systems, in a way that will be explained subsequently, we will not worry about this property of our construction here. We call the PEPS constructed in Eq. (7) “fixed-point” PEPS because they appear as special points within SPT phases, such as the AKLT state [57] within the Haldane phase. However, they are not necessarily the fixed-point of some renormalization transformation.

The construction in Eq. (7) may seem ad-hoc. Indeed, there are many ways we could construct a PEPS from an MPU that would lead to the same conclusions we find, such as replacing the Pauli Z in Eq. (7) with an X or Y . We chose this construction because it leads to familiar states for certain QCA, and for its simplicity. We will discuss this ambiguity further in Sec. III, and in Sec. V we will construct our PEPS in a different way than in Eq. (7).

It is important to stress how the term quasi-1D system is used here: The mapping to a *quasi-1D* system occurs by putting our PEPS on a long, skinny torus, and blocking tensors \mathcal{A}_T into rings along the skinny direction of the torus, giving rise to an effectively one-dimensional system,



The resulting ring tensor, denoted by \mathcal{A}_T , becomes the tensor of a *matrix product state (MPS)* [58] representation of a quasi-1D system. Throughout this paper, we consider systems that admit a quasi-1D representation with *injective* MPS tensors \mathcal{A} . This condition means that, for sufficiently large l , the set of products $\{\mathcal{A}^{i_1} \dots \mathcal{A}^{i_l}\}$ spans the space of all matrices of the same size [58]. Physically, injectivity means that the (quasi-)1D system has a finite correlation length.

For clarity, we use thicker lines when graphically representing MPS tensors like \mathcal{A}_T which represent blocked tensors. As follows straightforwardly from the definition (Eqs. (7,8)), the tensor \mathcal{A}_T has the symmetries

$$X_i \begin{array}{c} | \\ \square_{\mathcal{A}_T} \end{array} = \begin{array}{c} X_i \\ | \\ \square_{\mathcal{A}_T} \end{array} T(X_i), \quad Z_i \begin{array}{c} | \\ \square_{\mathcal{A}_T} \end{array} = \begin{array}{c} | \\ \square_{\mathcal{A}_T} \end{array} T(Z_i). \quad (9)$$

That is, a virtual Z passes through each ring freely and is transformed by the QCA T , while a virtual X passes through with the help of a physical X operator. Now, if T represents a CQCA, $T(Z_i)$ and $T(X_i)$ are products of Pauli operators. Hence, they can be pushed through the next ring of tensors as well, with the help of more physical X operators. Since we impose periodic boundary conditions, the CQCA will have a finite period L such that $t^L = \mathbb{I}$. In general, L is a complicated function of the circumference N of the torus, a point which we will return to later. If we push any Pauli operator in the virtual space through L rings of the PEPS, it will be mapped to itself, leading to the symmetry

$$\begin{array}{c} u(\xi) \quad u(t\xi) \quad u(t^2\xi) \quad \dots \quad u(t^{L-1}\xi) \\ \square_{\mathcal{A}_T} \quad \square_{\mathcal{A}_T} \quad \square_{\mathcal{A}_T} \quad \dots \quad \square_{\mathcal{A}_T} \end{array} = \begin{array}{c} V(\xi) \quad \square_{\mathcal{A}_T} \quad \square_{\mathcal{A}_T} \quad \dots \quad \square_{\mathcal{A}_T} \quad V(\xi)^\dagger \end{array}, \quad (10)$$

for all $\xi \in \mathbb{Z}_2^N \times \mathbb{Z}_2^N$, where

$$u(\xi) := \bigotimes_{i=1}^N X_i^{\xi_i^X}, \quad (11)$$

and $V(\xi) := \bigotimes_{i=1}^N X_i^{\xi_x} Z_i^{\xi_z}$. Hence, if we put our PEPS on a torus of dimension $N \times kL$, $k \in \mathbb{N}$, it will be invariant under the symmetry $\xi \mapsto U_T(\xi)^{\otimes k}$, where

$$U_T(\xi) := u(\xi) \otimes u(t\xi) \otimes \cdots \otimes u(t^{L-1}\xi). \quad (12)$$

We restrict to CQCA T such that $\xi \mapsto U_T(\xi)$ is a faithful representation of $\mathbb{Z}_2^N \times \mathbb{Z}_2^N$. This is necessary for the tensor \mathcal{A}_T to be injective, which we require to prove all major results in this paper.

The unitary $U_T(\xi)$ is more general than the usual global on-site symmetry. Rather than acting the same way on each site in the lattice, the representation “cycles” with a period L . We call such symmetries that are invariant under translation by L (but no fewer) sites “ L -cycle symmetries” [59]. If we block our PEPS into large blocks of size $N \times L$, $U_T(\xi)^{\otimes k}$ becomes a standard global symmetry. In this way, we can look at the conventional 1D SPT order protected by $U_T(\xi)$. Since $\xi \mapsto V(\xi)$ forms a projective representation of $\mathbb{Z}_2^N \times \mathbb{Z}_2^N$, our PEPS has non-trivial quasi-1D SPT order with respect to this symmetry [2].

Examples. Let us study some examples of the fixed-point PEPS we have constructed. First, consider the CQCA from Eq. (5). In this case, the state defined by Eq. (7) is the 2D cluster state (see Appendix A for a proof of this and of the following examples). The corresponding L -cycle symmetry has the form of cone-like operators with $L = N$, as pictured in Fig. 1. The SPT phase defined by these symmetries is exactly the cluster phase considered in Ref. [23]. For an example of a CQCA with fractal behavior, consider the CQCA T_f defined by the relations

$$T_f(X_i) = X_{i-1}Y_iX_{i+1}, T_f(Z_i) = X_i. \quad (13)$$

The fractal behavior of T_f has been demonstrated in Ref. [47]. This turns out to define the cluster state again, with the unitary

$$S = \begin{pmatrix} 1 & 0 \\ 0 & i \end{pmatrix} \quad (14)$$

applied to each site. So the cluster state also has fractal symmetries with Pauli- Y operators (since $SXS^\dagger = Y$). For a periodic CQCA, we choose the simple CQCA T_p to be

$$T_p(X_i) = Z_i, T_p(Z_i) = X_i. \quad (15)$$

This corresponds to a stack of decoupled 1D cluster states. These examples are all states that can be defined by a local stabilizer group, which is a feature common for any fixed-point PEPS constructed by Eq. (7), as is demonstrated in Appendix A. Hence, every state constructed by Eq. (7) is the unique ground state of a gapped, exactly solvable Hamiltonian.

III. SPT order with L -cycle symmetries

Above, we have used CQCA to define fixed-point PEPS with SPT order protected by subsystem symmetries. These

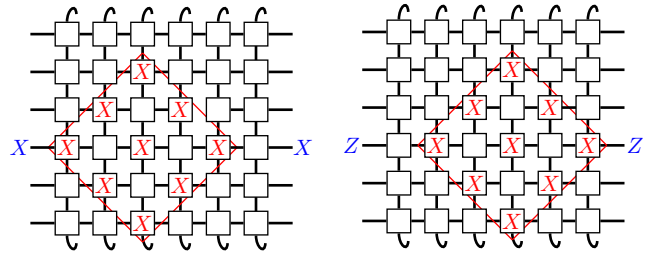


Figure 1. Two generators of the symmetries of the cluster phase defined by the CQCA T_g (Eq. (5)) on a torus of circumference $N = 6$. The other generators are vertical translates. In blue, the corresponding virtual representations for each generator are given.

symmetries have the form of L -cycle symmetries in the quasi-1D picture. We would now like to investigate the corresponding SPT phases that surround these fixed-points. It is important to note that these are indeed gapped phases of matter, since the fixed-point PEPS have gapped parent Hamiltonians (with a uniform gap $\Delta > 0$ that is independent of the system size, see Appendix A, as they are indeed stabilizer states).

A. L -cycle symmetries in MPS

To begin, we first need a better understanding of L -cycle symmetries in 1D systems. In general, we consider an MPS on a ring of length kL which is invariant under L -cycle symmetries of the form $U(g)^{\otimes k}|\psi\rangle = |\psi\rangle$ where

$$U(g) := u(g) \otimes u(\phi(g)) \otimes \cdots \otimes u(\phi^{L-1}(g)), \quad (16)$$

with $g \mapsto u(g)$ being a unitary representation of a group $G \ni g$, and ϕ an automorphism of G with $\phi^L = \mathbb{I}$. $g \mapsto u(g)$ alone need not be a faithful representation, but the whole cycle $U(g)$ should be faithful (otherwise G should be redefined such that $U(g)$ becomes faithful). The symmetries found in the previous section fall under this definition.

Again, we can block L consecutive sites into one larger site such that $U(g)^{\otimes k}$ acts in the same way on each block. If our state vector $|\psi\rangle$ is invariant under this symmetry, it is well-known that the blocked MPS tensors must satisfy the relation [60]

$$\begin{aligned} & u(g) \quad u(\phi(g)) \quad u(\phi^2(g)) \quad \cdots \quad u(\phi^{L-1}(g)) \\ & \begin{array}{c} | \\ \text{---} \mathcal{A} \text{---} \end{array} \begin{array}{c} | \\ \text{---} \mathcal{A} \text{---} \end{array} \begin{array}{c} | \\ \text{---} \mathcal{A} \text{---} \end{array} \cdots \begin{array}{c} | \\ \text{---} \mathcal{A} \text{---} \end{array} , \\ & = \\ & V(g) \begin{array}{c} | \\ \text{---} \mathcal{A} \text{---} \end{array} \begin{array}{c} | \\ \text{---} \mathcal{A} \text{---} \end{array} \begin{array}{c} | \\ \text{---} \mathcal{A} \text{---} \end{array} \cdots \begin{array}{c} | \\ \text{---} \mathcal{A} \text{---} \end{array} V(g)^\dagger . \end{aligned} \quad (17)$$

Therein, $g \mapsto V(g)$ is a projective representation of the group G , satisfying $V(g)V(h) = \omega(g, h)V(gh)$ for a cocycle ω [2]. The SPT order of $|\psi\rangle$ with respect to the symmetry $U(g)$ can be determined by ω [2]. For finite abelian groups, which we will focus on here, there is a particularly important type of

SPT phase called a maximally non-commutative phase [31]. These phases satisfy the property

$$\{g|\omega(g, h) = \omega(h, g) \forall h \in G\} = \{e\}, \quad (18)$$

and they have the largest edge-mode degeneracy of all phases for a given G [61]. Another important property of these phases is that $V(g)$ contains only one irrep $\tilde{V}(g)$, such that we have the decomposition

$$V(g) = \mathbb{I} \otimes \tilde{V}(g) \quad (19)$$

$\forall g \in G$ [62]. Our first technical result is the following theorem.

Theorem 1 (Normal form of MPS in maximally non-commutative SPT phase). *Any state vector $|\psi\rangle$ on a ring of length kL that is in a maximally non-commutative SPT phase with respect to an L -cycle symmetry representation (Eq. (16)) of a finite abelian group G admits an MPS representation of the form*

$$\mathcal{A}_{[j]}^i = B_{[j]}^i \otimes (C^i \Phi), \quad (20)$$

for suitable tensors $B_{[j]}^i$. Therein, $[j]$ is a site index such that $[j] = [j + L]$, Φ is uniquely defined by the relation $\tilde{V}(g) = \Phi^\dagger \tilde{V}(\phi(g)) \Phi$, and $C^i = \tilde{V}(g_i)$ for some $g_i \in G$. Throughout the phase, C^i and Φ remain constant, while $B_{[j]}^i$ varies.

This result is the essentially analagous to that given in Ref. [31] when extended to L -cycle symmetries. Φ and C^i are hence protected by the symmetry $g \mapsto U(g)$, in that they are present in a subspace of the virtual space of the MPS representation of all states in the phase. C^i are completely defined by the on-site representation $g \mapsto u(g)$ of Eq. 16, while the transformation Φ contains the information about the structure of the L -cycle symmetry. Hence, the same structure that defines the L -cycle symmetry also appears in the entanglement structure.

Proof. We now sketch the proof of Theorem 1, with full details given in Appendix B. The first step is to use the results of Ref. [63] to show that the symmetries of the block tensor (Eq. (17)) imply the following symmetries of the single tensor,

$$u(g) \begin{array}{c} \text{---} \\ | \\ \text{---} \\ \mathcal{A} \\ \text{---} \\ | \\ \text{---} \end{array} \propto V(g) \begin{array}{c} \text{---} \\ | \\ \text{---} \\ \mathcal{A} \\ \text{---} \\ | \\ \text{---} \end{array} V(\phi(g))^\dagger. \quad (21)$$

Using the fact that the SPT phase is maximally non-commutative, we can then rewrite this equation in the form

$$u(g) \begin{array}{c} \text{---} \\ | \\ \text{---} \\ \mathcal{A} \\ \text{---} \\ | \\ \text{---} \end{array} = \mathbb{I} \otimes \tilde{V}(g) \begin{array}{c} \text{---} \\ | \\ \text{---} \\ \mathcal{A} \\ \text{---} \\ | \\ \text{---} \end{array} \mathbb{I} \otimes \Phi^\dagger \Lambda^\dagger \tilde{V}(g)^\dagger \Lambda \Phi, \quad (22)$$

where Λ is a matrix that encodes the proportionality constant that hides in Eq. (21), hence it is not consistent throughout the

phase. From this, we can continue as in Ref. [31] to constrain the tensor \mathcal{A}^i into the form

$$\mathcal{A}^i = B^i \otimes (C^i \Lambda \Phi). \quad (23)$$

Finally, we can get rid of the non-universal Λ at the cost of losing full translation invariance of our MPS representation, and we are left with Eq. (20). \square

We can now apply Theorem 1 to the constructions found in the previous section. Given a CQCA T , we get a fixed-point PEPS which is in a non-trivial quasi-1D SPT phase with respect to the L -cycle symmetry $\xi \mapsto U_T(\xi)$ for $\xi \in \mathbb{Z}_2^N \times \mathbb{Z}_2^N$. Since $V(\xi)$ are N -qubit Pauli operators, it follows that this SPT phase is maximally non-commutative. Hence, Theorem 1 applies, and if we consider an arbitrary state within this SPT phase, it admit a quasi-1D MPS representation of the form Eq. (20), which in this case takes the form

$$\mathcal{A}_{[j]}^{\mathbf{i}} = \mathcal{B}_{[j]}^{\mathbf{i}} \otimes (C^{\mathbf{i}} T), \quad (24)$$

where $\mathbf{i} = (i_1, i_2, \dots, i_N)$ denotes the state of the N spins along a ring with $i = 0$ (1) corresponding to the vectors $|+\rangle$ ($|-\rangle$), and $C^{\mathbf{i}} = \otimes_{k=1}^N (Z_k)^{i_k}$. Notice that $C^{\mathbf{i}} T = \mathcal{A}_T^{\mathbf{i}}$, where \mathcal{A}_T is the tensor defined by Eqs. (7) and (8).

Thus, when CQCA are used to define subsystem symmetries, the presence of non-trivial SPT order under those symmetries is equivalent to the presence of the CQCA on the virtual level of the tensor network. This shows that the same structure appearing in the subsystem symmetry also appears in the entanglement structure found throughout the phase. This correspondence between QCA and subsystem SPT order is the first major result of this work.

B. Physical content of Eq. (24)

From Eq. (24), we see that the phases we define are characterized by both the tensor C^i and the CQCA T . What is the relative importance of these objects in determining the physics within the corresponding phase of matter?

Before we answer this, it is necessary to point out a fundamental difference between phases of matter from the perspective of quantum computation, and from the perspective of condensed matter physics. The SPT phases we consider here are defined by the symmetry group $\mathbb{Z}_2^N \times \mathbb{Z}_2^N$, the condition of maximal non-commutativity, and the representation $U_T(\xi)$. Here, we choose to include the representation $U_T(\xi)$ in the definition of the phase because states with the same SPT order but different symmetry representations can have different computational power [34], and we want to identify phases in which computational power is uniform.

From the condensed matter perspective, however, the physical representation is not as important in defining a phase of matter. This is because states with different symmetry representations can be smoothly interpolated between without closing the gap, hence they would be said to belong to the same phase [2, 3]. However, we must take caution in interpolating in this way between different representations $U_T(\xi)$. The problem is in the locality of the interpolation. $U_T(\xi)$ acts on

large blocks of size $N \times L$. Interpolating between different $U_T(\xi)$ thus results in a non-local transformation within each block, which violates the fundamental assumption of locality that is used to define phases of matter. We can, however, change the on-site representation $u(\xi)$ of our symmetry, since the resulting interpolation is local, provided that $u(\xi)$ remains a product of local operators. A change in T , on the other hand, results in a non-local transformation.

So if we were to temporarily adopt the condensed matter perspective, we see that changing $u(\xi)$, and hence C^i , does not change the phase of matter, while changing T may in general. We have such an example in the previous section already: defining $U_T(\xi)$ from the CQCA T_p (Eq. (15)) leads to an SPT phase built around a stack of decoupled 1D chains, while the phase defined by the CQCA T_g (Eq. (5)) is built around the 2D cluster state. These two phases are physically distinct, as discussed in Ref. [19]. This would still be true no matter how $u(\xi)$ is chosen. Hence, we conclude that the CQCA T is the principal ingredient in determining the physics of the phases of matter we have defined.

For the purposes of computation, however, we will however retain our definition of phases, in which different physical representations correspond to different phases of matter. This is because the precise form of C^i , which depends on $u(\xi)$, is crucial for the computational scheme we define in Sec. V. This should not be surprising, as almost all results relating SPT order to quantum computation assume a specific physical representation of the symmetry [22, 23, 29–32, 36–40].

Finally, we note that all phases we construct are maximally non-commutative quasi-1D SPT phases of $\mathbb{Z}_2^N \times \mathbb{Z}_2^N$. This means that they protect zero-energy edge modes of dimension 2^N [61]. This exponentially growing edge degeneracy was noted in Refs. [19, 22] as a signature of SPT phases protected by subsystem symmetries. In Sec. V, we encode logical information in these protected edge modes, such that computation proceeds almost identically for every state in a given phase.

IV. Relation to subsystem SPT order

The phases that we have considered until this point are quasi-1D SPT phases. We now relate them to genuine 2D SPT phases. Let us be clear about what is meant by quasi-1D SPT order and how it differs from a genuine 2D SPT order. The difference is in the notion of locality: SPT order is defined as equivalence classes of states under local, finite depth quantum circuits which respect the symmetry [4]. Such a circuit corresponds to a quasi-adiabatic evolution along a path of gapped, local Hamiltonians [64]. Here, ‘local’ depends on the dimensionality of the system. For our quasi-1D scenario, the evolution must be local between different rings of the torus (the long direction of the torus), but it may be non-local along the rings (the skinny direction around the torus). When we promote to a true 2D notion of locality, we enforce locality in both directions. This means that, for a given symmetry, the 2D phase is contained within the quasi-1D phase, so the results of the previous section also hold throughout the corresponding 2D phase defined by the same symmetries.

			$T(Z)$	Z		
		$T(Z)$	Z	$T(Z)$	Z	
Z	$T(Z)$	Z	$T(Z)$	Z	$T(Z)$	Z
		$T(Z)$	Z	$T(Z)$	Z	
			$T(Z)$	Z		

(a)

		$T(Z)$	Z			
	$T(Z)$	Z				
$T(Z)$	Z					$T(Z)$
Z					$T(Z)$	Z
				$T(Z)$	Z	
			$T(Z)$	Z		

(b)

Figure 2. Representation of the general appearance of lines and cones in glider CQCA, for $c = 1$. Each column represents a product of Pauli operators on $N = 6$ qubits with periodic boundaries, and advancing to the right is equivalent to one application of T . After 6 steps, any operator returns to itself.

It is important to stress the the new 2D situation again constitutes a proper phase of matter, in that it embodies all states that can be reached from the fixed point states via local quantum circuits that respect the symmetry. Using the techniques of Refs. [65, 66], one can show a lower bound to the gap of the parent Hamiltonian in a vicinity of the fixed point model.

We now show that, in the case of glider CQCA, promoting to a 2D notion of locality allows us to equivalently define our phases in terms of rigid line-like symmetries acting on 1D subsystems. In general, the symmetries defined by glider CQCA are shaped like cones. This follows from Eq. (6) which, for glider CQCA, takes the form $t^2 = (u^c + u^{-c})t + \mathbb{I}$. Thus, if we apply T to any single-qubit Pauli P_i , we find

$$T(T(P_i)) = T^2(P_i) = T(P_{i-c})P_iT(P_{i+c}).$$

We can continue in this fashion, and we see that powers of T can be expressed as cones which expand until they wrap all the way around the torus, after which they contract back to a point (see Fig. 2(a) for the case $P_i = Z_i$).

This picture also gives us an easy way to understand the existence of gliders, see Fig. 2(b). The gliders lead to line-like symmetries of the state, as pictured in Fig. 3. The line symmetries can be generated as products of the cone symmetries, but the converse is not true on a finite torus. Indeed, the line symmetries form a \mathbb{Z}_2^{N-2} subgroup of the full \mathbb{Z}_2^N symmetry group of cones in the cluster phase.

The claim is that, when a 2D notion of locality is enforced, the line symmetries defined by gliders are sufficient to protect the SPT order. Fig. 2(b) shows that the operator $T(Z_i)Z_{i-1}$ defines a glider and hence a line symmetry. Likewise, $Z_iT(Z_{i-1})$ defines a glider moving in the opposite direction. Now, for any even integer k , we can write

$$Z_i \otimes Z_{i-k} = (Z_iT(Z_{i-1}))(T(Z_{i-1})Z_{i-2}) \dots (T(Z_{i-k+1})Z_{i-k}).$$

That is, we can write a product of non-neighbouring Z 's as a product of gliders. Since Z_i in the virtual space corresponds

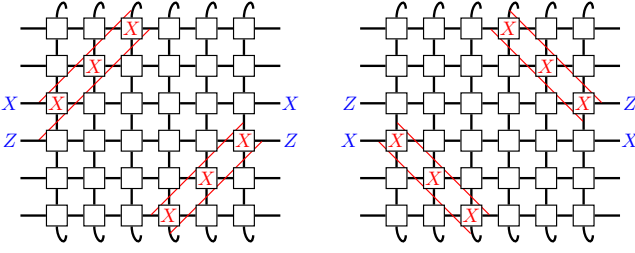


Figure 3. The gliders of a CQCA define line-like symmetries of the PEPS, as pictured here for the CQCA T_g of Eq. (5) which defines the cluster phase. Operators in blue show the corresponding representation in the virtual space.

to a cone symmetry in the physical space, we see that we can create pairs of cone symmetries with products of line symmetries. The same argument can be repeated for X_i in place of Z_i .

If we separate these cones sufficiently far from each other, then each local gate in the finite depth quantum circuit will see only one of the cones. So a local gate that is symmetric under the line symmetries is also symmetric under the cone symmetries. Since we require in the definition of SPT order that each *local* gate of the finite depth quantum circuit commutes with the symmetry, this implies that a circuit which is symmetric under the line symmetries is also symmetric under the cone symmetries. Therefore, the 2D phase defined by line symmetries is contained within the quasi-1D phase defined by the cone symmetries.

Defining an SPT phase by symmetries acting on lower-dimensional lines has been done in Refs. [19, 23, 67], and in Ref. [19] such phases have been dubbed “*subsystem*” SPT (SSPT) phases. Hence, the SPT phases we defined here can be considered SSPT phases whenever the CQCA supports gliders, and the line symmetries are the fundamental symmetries defining the phases. When the CQCA is periodic, the cone symmetries are themselves line symmetries, but they act in the horizontal direction of the torus, rather than diagonally as in the glider case. These phases are like the “weak-SSPT” phases defined in Ref. [19]. When the CQCA is fractal, we do not have line-like symmetries [47], and we must treat the fractal symmetries themselves as fundamental. This leads to a definition of 2D phases via fractal symmetry operators, as in Refs. [16, 22].

V. Computational power of the QCA phases

Now that we have defined 2D SPT phases via CQCA, and we have understood the basic properties of these phases, we move on to characterizing their computational power. In this section, we will prove our second main result:

Theorem 2 (Computational phases of matter). *For every glider CQCA and fractal CQCA, there exists a 2D SPT phase in which every state is a resource for universal MBQC, except for a possible subset of zero measure. Furthermore, the universal circuit model is simulated with polynomial overhead.*

The SPT phases for which we prove this theorem are slightly different from the ones considered so far. In order to prove universality in a straightforward manner, we redefine our fixed-point PEPS in terms of a two-qubit unit cell, labelling the two qubits within a unit cell by a and b . The new fixed-point PEPS is defined by a local tensor A'_T whose components are given by

$$\begin{aligned} |{++}\rangle & \quad |{-+}\rangle \\ \begin{array}{c} \text{---} \\ | \\ \text{---} \end{array} A'_T \begin{array}{c} \text{---} \\ | \\ \text{---} \end{array} & := \begin{array}{c} \text{---} \\ | \\ \text{---} \end{array} \mathcal{T} \begin{array}{c} \text{---} \\ | \\ \text{---} \end{array}, & \quad \begin{array}{c} \text{---} \\ | \\ \text{---} \end{array} A'_T \begin{array}{c} \text{---} \\ | \\ \text{---} \end{array} & := \begin{array}{c} \text{---} \\ | \\ \text{---} \end{array} \textcircled{Z} \mathcal{T} \begin{array}{c} \text{---} \\ | \\ \text{---} \end{array}, \\ |{+-}\rangle & \quad |{--}\rangle \\ \begin{array}{c} \text{---} \\ | \\ \text{---} \end{array} A'_T \begin{array}{c} \text{---} \\ | \\ \text{---} \end{array} & := \begin{array}{c} \text{---} \\ | \\ \text{---} \end{array} \textcircled{X} \mathcal{T} \begin{array}{c} \text{---} \\ | \\ \text{---} \end{array}, & \quad \begin{array}{c} \text{---} \\ | \\ \text{---} \end{array} A'_T \begin{array}{c} \text{---} \\ | \\ \text{---} \end{array} & := \begin{array}{c} \text{---} \\ | \\ \text{---} \end{array} \textcircled{XZ} \mathcal{T} \begin{array}{c} \text{---} \\ | \\ \text{---} \end{array}, \end{aligned} \quad (25)$$

where \mathcal{T} is again the MPU representation of the CQCA. The states defined by Eq. (25) are again stabilizer states. Hence, they are unique ground states of gapped Hamiltonians.

The tensors A'_T can be used to define the ring tensor \mathcal{A}'_T as in Eq. (8). Proceeding from here in the same way as the qubit case, we can construct an L -cycle symmetry representation

$$\xi \mapsto U'_T(\xi) = u'(\xi) \otimes u'(t\xi) \otimes \cdots \otimes u'(t^{L-1}\xi) \quad (26)$$

of $\mathbb{Z}_2^N \times \mathbb{Z}_2^N$, where the on-site representation is defined by

$$u'(\xi) = \bigotimes_{i=1}^N X_i^{a\xi_i^X} X_i^{b\xi_i^Z}, \quad (27)$$

where X_i^a, X_i^b denotes the Pauli-X matrix acting on the qubit a and b at site i , respectively. Again, the resulting state has non-trivial SPT order under this L -cycle symmetry, and we can prove that Eq. (24) holds throughout the corresponding SPT phase, where C^i can now be any N -qubit Pauli, not just a product of Z 's.

We can briefly compare this to the original qubit construction of Eq. (7). By changing the way we constructed our PEPS, we have only changed the representation $u \mapsto u'$, as seen in Fig. 4. As discussed in Sec. III, we therefore expect these phases with a two qubit unit cell to be physically similar to those we constructed originally. Nevertheless, there is a distinction in their use for MBQC due to the different C^i appearing in Eq. (24).

A. MBQC in SPT phases of matter

To prepare for the proof of Theorem 2, we require a number of technical results. We begin with a very brief review of the constructions in Refs. [23, 34, 35] which show how an SPT phase can be used as a resource for MBQC. There are three key features of the constructions which are relevant to the current work:

1. Logical qubits are encoded in the virtual space of the tensor network [26, 27]. Specifically, N qubits are encoded in the 2^N -dimensional subspace of Eq. (24)

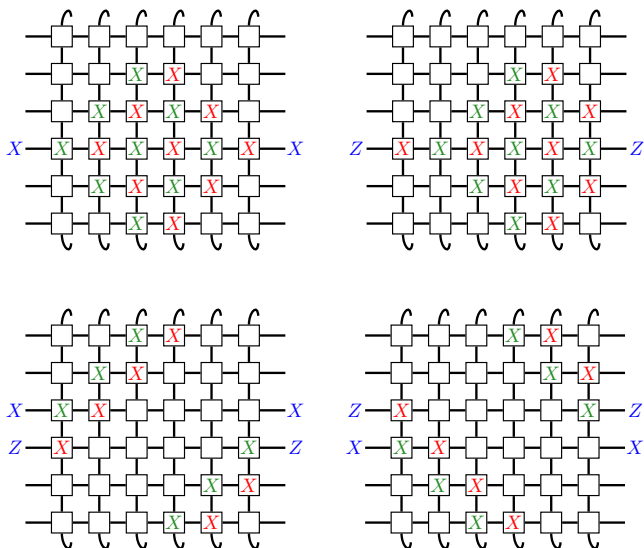


Figure 4. The modified line and cone symmetries arising from the cluster CQCA T_g of Eq. (5) when using the two qubit per-site construction. Green (red) X's denote the Pauli-X operator acting on qubit a (b) on a given site, while blue operators show the corresponding virtual representation. Note that the analysis in Sec. IV still holds in this case: the line symmetries, although widened, are still sufficient to protect the phase.

which is uniform throughout the corresponding SPT phase. One time-step of the computation is enacted by measuring every qubit in a *block* consisting of L consecutive rings around the torus, where L is the period of the CQCA. Information can be initialized into this space and subsequently read-out by appropriate measurement patterns on blocks.

2. Logical gates are performed by measuring a single qubit in a block in a perturbed basis

$$\{|+\rangle + i\alpha|-\rangle, |-\rangle - i\alpha|+\rangle\}, \quad (28)$$

and measuring the rest of the qubits in a block in the basis $\{|+\rangle, |-\rangle\}$. According to Eq. (24), and the computational scheme of Ref. [35], if the qubit measured in the basis in Eq. (28) is located at site (n, l) in the block, the corresponding logical gate is, up to second order in $d\alpha$,

$$R_{(n,l)}(d\alpha) = \exp(2id\alpha\nu_{(n,l)}T^{L-l+1}(P_n)), \quad (29)$$

where P_n is the Pauli X or Z operator acting on logical qubit n , depending if we measure the first or second qubit at site (n, l) in the basis Eq. (28), respectively. $\nu_{(n,l)}$ are a set of constants that characterize the part of the state that is not uniform within the SPT phase. These constants can be measured before computation and accounted for (and thereby ignored) by adjusting $d\alpha$ unless they are equal to 0, in which case computation fails. This only occurs for a subset of states of zero measure. The full set of gates we can implement is given by the Lie group $\mathcal{L}_T = \exp(i\mathcal{O}_T)$ where \mathcal{O}_T

is the Lie algebra generated by the set $\{T^l(Z_n)|l = 1 \dots L, n = 1 \dots N\}$ with linear combinations and the matrix commutator. \mathcal{L}_T is the same for every state in the SPT phase defined by the CQCA T .

3. Every non-trivial gate must be followed up by measuring a large number of blocks in the $\{|0\rangle, |1\rangle, |2\rangle\}$ basis. The number of blocks measured is on the order of the correlation length of the system (in the long direction). This serves to decouple the two virtual subspaces in Eq. (24), which become slightly entangled after a logical gate.

All that remains is to determine the period L of the CQCA which determines the length of a single step of computation, and the group of gates \mathcal{L}_T .

B. Period of the CQCA

We first determine the period of our CQCA. We recall the matrix representation t of the CQCA. The task is then to determine the smallest L such that $t^L = \mathbb{I}$, which we do by invoking Eq. (6). Since the trace of the CQCA appears in the equation, the analysis now splits into three parts, depending on whether the CQCA is of periodic, glider, or fractal type.

Periodic CQCA. For periodic CQCA, we have either $\text{Tr}(t) = a$, where $a = 0, 1$. Using Eq. (6), it is easy to check that the period is then $L = a + 2$ [47]. Note that this period is independent of the circumference N . In particular, the CQCA is periodic even on an infinite chain, while the glider and fractal CQCA are only periodic when periodic boundary conditions are enforced. This is the reason why only these CQCA are called “periodic”.

Glider CQCA. For CQCA that support gliders, the period can be determined from the cone structure in Fig. 2(a). For $c=1$ and N even, this cycle takes N steps (for odd N , it takes $2N$ steps, but we only consider N even). For $c > 1$, the above is still true, but there may be a smaller number L also satisfying $t^L = \mathbb{I}$. We ignore this possibility for simplicity. Thus, the period of a glider CQCA on a ring of circumference $2N$ can always be taken to be $L = 2N$.

Fractal CQCA. For CQCA with fractal behavior, the case is more complicated. Indeed, due to their fractal nature, the period L of these CQCA can be a wildly fluctuating function of N . In fact, $L(N)$ can appear to have exponentially growing behavior (see Appendix C for an example). This would pose a significant problem to computation. Since N is essentially our number of qubits, and L controls the duration of a single step of computation, an exponential relationship implies that computation time scales exponentially with the number of qubits. Thus we could not call the resulting computational scheme universal, even if we have a full set of gates.

Luckily, it turns out that this problem can be avoided. Indeed, although $L(N)$ may have an exponential envelope, it

turns out that there is a subsequence of system sizes for which the relationship is linear. Specifically, when $N = 2^k$, we have either $L = 2^k = N$ or $L = 2^k + 2^{k-1} = \frac{3}{2}N$. This behavior can be seen for the CQCA defined in Eq. (13), as shown in Appendix C which also contains the general proof.

C. Determining gate set

We must now determine the Lie group of gates \mathcal{L}_T . In the following, we construct a universal set of gates as long as T is a CQCA of glider or fractal type. To construct a universal set of gates, notice first that we trivially have all single-qubit gates by setting $l = 1$ in Eq. (29) (this would not be true for the original qubit construction Eq. (7), complicating matters in that case significantly). Thus, if we can construct any two-qubit entangling gate, we will have a full gate set [68]. In Ref. [23], a two-qubit gate was constructed from a three-qubit gate by initialising one qubit into a particular eigenstate on which the three-qubit gate acts trivially. Here, we will employ a similar technique.

Consider $T(Z_i)$, for any i . Assume that $T(Z_i)$ “spreads”, meaning that it has support outside of site i . If this is not the case, then we can instead follow through with the argument using $T^{L-1}(Z_i) = T^{-1}(Z_i)$, since Eq. (6) tells us that $t^{-1} = t + \text{Tr}(t)\mathbb{I}$, so either $T(Z_i)$ or $T^{-1}(Z_i)$ spreads as long as $\text{Tr}(t)$ is not a constant, meaning T is of either glider or fractal type.

If $T(Z_i)$ spreads, it will be a product of Pauli operators supported on the interval $[i - n, i + n]$, for some minimal n , which is symmetric about site i . The trick now is to make every $2n$ -th qubit a logical qubit, and initialize the qubits in between each logical qubit into the $+1$ eigenstate of the middle $2n - 1$ operators in $T(Z_i)$. This initialization can always be done since we have all single qubit gates at our disposal, as described in Ref. [23]. Then, $T(Z_i)$ will act as a two-qubit gate on logical qubits at positions $i - n$ and $i + n$ while leaving the qubits in between unchanged. Hence we get a non-trivial two-qubit entangling gate on all neighbouring pairs of logical qubits which, together with the single-qubit gates, form a universal set.

For an explicit example, consider the CQCA with $T(Z_i) = Z_{i-2}X_{i-1}Z_iX_{i+1}Z_{i+1}$. If the qubits at positions 1 and 5 are logical qubits, then we put the qubits at positions 2, 3, and 4 in states $|+\rangle$, $|0\rangle$, and $|+\rangle$, respectively. Then the gate $\exp(2id\alpha T(Z_3))$ reduces to $\exp(2id\alpha Z_1Z_5)$, which is an entangling gate on the logical qubits.

D. Proving computational universality

We now have all of the ingredients needed to prove Theorem 2.

Proof of Theorem 2. Based on the above discussions, we see that a) N can always be scaled in such a way that the period L is linear in N , and b) we can construct a universal set of gates on $q = \lfloor N/2n \rfloor$ qubits for a fixed n , *i.e.* $SU(2^q) \subset \mathcal{L}_T$.

Finally, the computational scheme of Refs. [23, 34, 35] which we employ here has polynomial overhead for logical gates. Thus, overall, we can perform universal quantum computation on q logical qubits in $\text{poly}(q)$ time, as stated in the theorem. \square

Note that our proof does not apply to periodic CQCA, and there are examples of periodic CQCA which do not lead to universal phases. Consider again the CQCA in Eq. (15), which is periodic and describes decoupled 1D chains. Such a system cannot be a universal resource for measurement-based quantum computation with our methods, since we cannot create entangling gates with local measurements.

In order to obtain a universal set of gates straightforwardly, we had to modify our original construction to one with two qubits per site. We can also ask if a universal set of gates can be obtained without this redefinition. This is sometimes possible, and the cluster phase in Ref. [23] is an example. Our fractal CQCA in Eq. (13) is another example, as can be shown using the same proof as in Ref. [23]. On the other hand, there are some CQCA for which the qubit construction of Eq. (7) does not appear lead to a computationally universal phase. We note that, in Ref. [41], two more computationally universal phases with fractal symmetries were recently constructed, one based on the cluster state on the honeycomb lattice. These phases were also defined with respect to a two qubit unit cell.

VI. Conclusions

In this work, we have used quantum cellular automata to define subsystem symmetries and SPT phases of matter. We have characterized which of the resulting phases of matter are computationally universal from the perspective of measurement-based quantum computation. The relation we uncovered between QCA and SPT order protected by subsystem symmetries in tensor networks should aid in the understanding and classification of these relatively novel phases of matter.

The next step in classifying these phases would be to make further use of tensor network language. In Ref. [23], it was shown that subsystem SPT order is associated with a set of symmetries of a single tensor. The ring symmetries considered here can be easily used to determine the symmetries of the single tensor as well. Examining the symmetries of a single tensor has proven useful for classifying phases of matter in the past [2, 3, 69–71], so it is likely this will be the case for subsystem symmetries as well.

One immediate generalization of our result is to go beyond logical qubits. Here, we considered QCA acting only on systems of qubits, but we could extend this to systems of arbitrary local dimension d . In this case, we could realize systems with subsystem symmetry groups of the form $(G \times G)^N$ for arbitrary abelian G , and our analysis would be in terms of generalized Pauli and Clifford operators [51]. This extension would be useful for the classification of subsystem SPT phases, and would also lead to new computationally universal phases. Our general formalism in Sec. III is already equipped to handle this generalization.

VII. Acknowledgements

This work is supported by the NSERC (DTS, RR), Cifar (RR), the Stewart Blusson Quantum Matter Institute (RR), the

ERC TAQ (JBV, JE), the DFG CRC 183 (JE), the Templeton Foundation, and the Austrian Science Fund FWF within the DK-ALM: W1259-N27 (HPN). DTS thanks N. Schuch for discussions, and H. Dreyer for discussions and help in preparation of the manuscript.

-
- [1] F. Pollmann, A. M. Turner, E. Berg, and M. Oshikawa, *Phys. Rev. B* **81**, 064439 (2010).
- [2] N. Schuch, D. Pérez-García, and I. Cirac, *Phys. Rev. B* **84**, 165139 (2011).
- [3] X. Chen, Z.-C. Gu, and X.-G. Wen, *Phys. Rev. B* **83**, 035107 (2011).
- [4] X. Chen, Z.-C. Gu, Z.-X. Liu, and X.-G. Wen, *Phys. Rev. B* **87**, 155114 (2013).
- [5] T. Senthil, *Ann. Rev. Cond. Mat. Phys.* **6**, 299 (2015).
- [6] A. Nietner, C. Krumnow, E. J. Bergholtz, and J. Eisert, *Phys. Rev. B* **96**, 235138 (2017).
- [7] C. L. Kane and E. J. Mele, *Phys. Rev. Lett.* **95**, 146802 (2005).
- [8] I. Affleck, *J. Phys. Cond. Mat.* **1**, 3047 (1989).
- [9] F. Pollmann, E. Berg, A. M. Turner, and M. Oshikawa, *Phys. Rev. B* **85**, 075125 (2012).
- [10] H. Song, S.-J. Huang, L. Fu, and M. Hermele, *Phys. Rev. X* **7**, 011020 (2017).
- [11] R. Thorngren and D. V. Else, *Phys. Rev. X* **8**, 011040 (2018).
- [12] S.-J. Huang, H. Song, Y.-P. Huang, and M. Hermele, *Phys. Rev. B* **96**, 205106 (2017).
- [13] D. Gaiotto, A. Kapustin, N. Seiberg, and B. Willett, *J. High En. Phys.* **2015**, 172 (2015).
- [14] S. Vijay, J. Haah, and L. Fu, *Phys. Rev. B* **94**, 235157 (2016).
- [15] B. Yoshida, *Phys. Rev. B* **93**, 155131 (2016).
- [16] A. Kubica and B. Yoshida, (2018), [arXiv:1805.01836](https://arxiv.org/abs/1805.01836).
- [17] S. Roberts, B. Yoshida, A. Kubica, and S. D. Bartlett, *Phys. Rev. A* **96**, 022306 (2017).
- [18] S. Roberts and S. D. Bartlett, (2018), [arXiv:1805.01474](https://arxiv.org/abs/1805.01474).
- [19] Y. You, T. Devakul, F. J. Burnell, and S. L. Sondhi, (2018), [arXiv:1803.02369](https://arxiv.org/abs/1803.02369).
- [20] Y. You, T. Devakul, F. J. Burnell, and S. L. Sondhi, (2018), [arXiv:1805.09800](https://arxiv.org/abs/1805.09800).
- [21] D. J. Williamson, *Phys. Rev. B* **94**, 155128 (2016).
- [22] T. Devakul, Y. You, F. J. Burnell, and S. L. Sondhi, (2018), [arXiv:1805.04097](https://arxiv.org/abs/1805.04097).
- [23] R. Raussendorf, C. Okay, D.-S. Wang, D. T. Stephen, and H. Poulsen Nautrup, (2018), [arXiv:1803.00095](https://arxiv.org/abs/1803.00095).
- [24] R. Raussendorf and H. J. Briegel, *Phys. Rev. Lett.* **86**, 5188 (2001).
- [25] R. Raussendorf, D. E. Browne, and H. J. Briegel, *Phys. Rev. A* **68**, 022312 (2003).
- [26] D. Gross and J. Eisert, *Phys. Rev. Lett.* **98**, 220503 (2007).
- [27] D. Gross, J. Eisert, N. Schuch, and D. Perez-Garcia, *Phys. Rev. A* **76**, 052315 (2007).
- [28] A. C. Doherty and S. D. Bartlett, *Phys. Rev. Lett.* **103**, 020506 (2009).
- [29] A. Miyake, *Phys. Rev. Lett.* **105**, 040501 (2010).
- [30] S. D. Bartlett, G. K. Brennen, A. Miyake, and J. M. Renes, *Phys. Rev. Lett.* **105**, 110502 (2010).
- [31] D. V. Else, I. Schwarz, S. D. Bartlett, and A. C. Doherty, *Phys. Rev. Lett.* **108**, 240505 (2012).
- [32] J. Miller and A. Miyake, *Phys. Rev. Lett.* **114**, 120506 (2015).
- [33] D.-S. Wang, D. T. Stephen, and R. Raussendorf, *Phys. Rev. A* **95**, 032312 (2017).
- [34] D. T. Stephen, D.-S. Wang, A. Prakash, T.-C. Wei, and R. Raussendorf, *Phys. Rev. Lett.* **119**, 010504 (2017).
- [35] R. Raussendorf, D.-S. Wang, A. Prakash, T.-C. Wei, and D. T. Stephen, *Phys. Rev. A* **96**, 012302 (2017).
- [36] H. Poulsen Nautrup and T.-C. Wei, *Phys. Rev. A* **92**, 052309 (2015).
- [37] J. Miller and A. Miyake, *Npj Quant. Inf.* **2**, 16036 (2016).
- [38] J. Miller and A. Miyake, *Phys. Rev. Lett.* **120**, 170503 (2018).
- [39] T.-C. Wei and C.-Y. Huang, *Phys. Rev. A* **96**, 032317 (2017).
- [40] Y. Chen, A. Prakash, and T.-C. Wei, *Phys. Rev. A* **97**, 022305 (2018).
- [41] T. Devakul and D. J. Williamson, (2018), [arXiv:1806.04663](https://arxiv.org/abs/1806.04663).
- [42] A. Kitaev, *Ann. Phys.* **303**, 2 (2003).
- [43] M. Freedman, A. Kitaev, M. Larsen, and Z. Wang, *Bull. Amer. Math. Soc.* **40**, 31 (2003).
- [44] C. Nayak, S. H. Simon, A. Stern, M. Freedman, and S. Das Sarma, *Rev. Mod. Phys.* **80**, 1083 (2008).
- [45] B. Schumacher and R. F. Werner, (2004), [arXiv:quant-ph/0405174](https://arxiv.org/abs/quant-ph/0405174).
- [46] D.-M. Schlingemann, H. Vogts, and R. F. Werner, *J. Math. Phys.* **49**, 112104 (2008).
- [47] J. Gütschow, S. Uphoff, R. F. Werner, and Z. Zimboras, *J. Math. Phys.* **51**, 015203 (2010).
- [48] J. I. Cirac, D. Perez-Garcia, N. Schuch, and F. Verstraete, *J. Stat. Mech.* **2017**, 083105 (2017).
- [49] J. C. Bridgeman and C. T. Chubb, *J. Phys. A* **50**, 223001 (2017).
- [50] D. Gottesman, in *Selected papers from the First NASA International Conference on Quantum Computing and Quantum Communications* (Springer, 1998) [quant-ph/9802007v1](https://arxiv.org/abs/quant-ph/9802007v1).
- [51] J. Bermejo-Vega and M. Van Den Nest, *Quant. Inf. Comp.* **14**, 181 (2014), [arXiv:1210.3637](https://arxiv.org/abs/1210.3637).
- [52] R. Raussendorf, *Phys. Rev. A* **72**, 052301 (2005).
- [53] J. Bermejo-Vega, D. Hangleiter, M. Schwarz, R. Raussendorf, and J. Eisert, *Phys. Rev. X* **8**, 021010 (2018).
- [54] A. Mantri, T. F. Demarie, and J. F. Fitzsimons, *Scientific Reports* **7**, 42861 EP (2017), article.
- [55] In Refs. [48, 72], QCA are assigned an index according to the amount of information flow to the left or right. Our restriction is to QCA with index 0.
- [56] F. Verstraete, V. Murg, and J. Cirac, *Adv. Phys.* **57**, 143 (2008).
- [57] I. Affleck, T. Kennedy, E. H. Lieb, and H. Tasaki, *Phys. Rev. Lett.* **59**, 799 (1987).
- [58] D. Perez-Garcia, F. Verstraete, M. M. Wolf, and J. I. Cirac, *Quant. Inf. Comp.* **7**, 401 (2007), [arXiv:0608197](https://arxiv.org/abs/0608197).
- [59] We note that a more general version of L -cycle symmetries are also being studied in Ref. [73].
- [60] D. Pérez-García, M. M. Wolf, M. Sanz, F. Verstraete, and J. I. Cirac, *Phys. Rev. Lett.* **100**, 167202 (2008).
- [61] I. Marvian, *Phys. Rev. B* **95**, 045111 (2017).
- [62] I. G. Berkovich and E. Zhmud, *Characters of finite groups*, Vol. 1 (American Mathematical Soc., 1998).
- [63] A. Molnar, J. Garre-Rubio, D. Perez-Garcia, N. Schuch, and J. I. Cirac, (2018), [arXiv:1804.04964](https://arxiv.org/abs/1804.04964).
- [64] X.-G. Wen, *Rev. Mod. Phys.* **89**, 041004 (2017).

- [65] B. Nachtergaele, *Commun. Math. Phys.* **175**, 565 (1996).
 [66] A. S. Darmawan and S. D. Bartlett, *New J. Phys.* **16**, 073013 (2014).
 [67] D. V. Else, S. D. Bartlett, and A. C. Doherty, *New J. Phys.* **14**, 113016 (2012).
 [68] M. A. Nielsen and I. Chuang, *Quantum computation and quantum information* (AAPT, 2002).
 [69] N. Schuch, I. Cirac, and D. Perez-Garcia, *Ann. Phys.* **325**, 2153 (2010).
 [70] D. J. Williamson, N. Bultinck, M. Mariën, M. B. Şahinoğlu, J. Haegeman, and F. Verstraete, *Phys. Rev. B* **94**, 205150 (2016).
 [71] A. Molnar, Y. Ge, N. Schuch, and J. I. Cirac, *J. Math. Phys.* **59**, 021902 (2018).
 [72] D. Gross, V. Nesme, H. Vogts, and R. F. Werner, *Commun. Math. Phys.* **310**, 419 (2012).
 [73] D. Sauerwein, A. Molnar, J. I. Cirac, and B. Kraus, (in preparation).

A. Stabilizers for fixed-point PEPS

In Sec. II, we build SPT phases around special fixed-point PEPS as defined by Eq. (7). In order to gain a better intuition and to construct gapped parent Hamiltonians, we show in this section that the fixed-point PEPS are also stabilizer states with local stabilizer groups. The fixed-point PEPS defined by Eq. (7) have more symmetries than those shown in Eq. (9). They also have the following symmetries,

$$Z_i \begin{array}{c} | \\ \text{---} \mathcal{A}_T \text{---} \\ | \end{array} = \begin{array}{c} Z_i \\ | \\ \text{---} \mathcal{A}_T \text{---} \\ | \end{array} = \begin{array}{c} | \\ \text{---} \mathcal{A}_T \text{---} \\ | \end{array} T(Z_i). \quad (\text{A1})$$

Note that these symmetries exist only at the fixed-point, and they do not persist throughout the corresponding SPT phase. In addition to these symmetries, we also need the identity from Eq. (6). In general, we have $\text{Tr}(t) = \sum_{k=1}^m \alpha_k (u^k + u^{-k}) + \beta$ for $\alpha_k, \beta \in \{0, 1\}$. Stated in terms of operators, Eq. (6) then tells us

$$T^2(Z_i) = Z_i \bigotimes_{k=1}^m [T(Z_{i-k})T(Z_{i+k})]^{\alpha_k} T(Z_i)^\beta. \quad (\text{A2})$$

Using Eqs. (9), (A1) and (A2), we can now determine the form of the stabilizers for our states,

$$\begin{aligned} \begin{array}{c} | \\ \text{---} \mathcal{A}_T \text{---} \\ | \end{array} \begin{array}{c} | \\ \text{---} \mathcal{A}_T \text{---} \\ | \end{array} \begin{array}{c} | \\ \text{---} \mathcal{A}_T \text{---} \\ | \end{array} &= \begin{array}{c} Z_i \\ | \\ \text{---} \mathcal{A}_T \text{---} \\ | \end{array} T(Z_i) \begin{array}{c} | \\ \text{---} \mathcal{A}_T \text{---} \\ | \end{array} \begin{array}{c} | \\ \text{---} \mathcal{A}_T \text{---} \\ | \end{array} \\ &= \begin{array}{c} Z_i \\ | \\ \text{---} \mathcal{A}_T \text{---} \\ | \end{array} u \left(t \begin{pmatrix} 0 \\ u^i \end{pmatrix} \right) \begin{array}{c} | \\ \text{---} \mathcal{A}_T \text{---} \\ | \end{array} T^2(Z_i) \begin{array}{c} | \\ \text{---} \mathcal{A}_T \text{---} \\ | \end{array} \\ &= \begin{array}{c} Z_i \\ | \\ \text{---} \mathcal{A}_T \text{---} \\ | \end{array} u \left(t \begin{pmatrix} 0 \\ u^i \end{pmatrix} \right) \cdot \bar{Z} \begin{array}{c} | \\ \text{---} \mathcal{A}_T \text{---} \\ | \end{array}. \end{aligned}$$

In the first equality, we have used Eq. (A1). In the second, we have employed Eq. (9) (note that Z_i is represented

as the polynomial vector $(0, u^i)$). In the third equality, we have used Eq. (A2), and Eq. (A1) to pull the Z_i and $\bar{Z} := \bigotimes_{k=1}^m [Z_{i-k}Z_{i+k}]^{\alpha_k} Z_i^\beta$ onto the physical legs. Since $u(\xi)$ is a localised product of X operators and \bar{Z} is a localised product of Z operators, we have derived a local stabilizer for each PEPS. We can similarly derive an independent stabilizer S_i for any site i in the lattice. One can easily check that, due to the reflection symmetry of the stabilizers, all stabilizers commute as needed. So the fixed-point PEPS is the unique ground state of the Hamiltonian

$$\mathcal{H} = - \sum_i S_i, \quad (\text{A3})$$

which is a local Hamiltonian with a uniform gap.

We can now verify the claimed examples in Section II. If we construct the stabilizers for the fixed-point PEPS defined by the CQCA T_g in Eq. (5), then we find that they have the following form,

$$\begin{array}{c} Z \\ S_i = Z X_i Z, \\ Z \end{array} \quad (\text{A4})$$

which is indeed the familiar form of the cluster stabilizer [25]. If we use the CQCA T_f in Eq. (13), we find

$$\begin{array}{c} Z \\ S_i = Z Y_i Z, \\ Z \end{array} \quad (\text{A5})$$

which corresponds to the cluster state with the operator

$$S = \begin{pmatrix} 1 & 0 \\ 0 & i \end{pmatrix} \quad (\text{A6})$$

applied to every site. Finally, with the CQCA T_p of Eq. (15), we get stabilizers with the simple form,

$$S_i = ZX_iZ, \quad (\text{A7})$$

which does indeed correspond to a stack of uncoupled 1D cluster states.

The fixed-point PEPS defined with respect to a two-qubit unit cell in Eq. (25) are also stabilizer states with a local stabilizer group, as can be straightforwardly shown in the same way as above. Hence, these fixed-point PEPS are also ground states of uniformly gapped Hamiltonians.

B. Cycle symmetries

Here we show how to constrain MPS tensors of states which have SPT order with respect to L -cycle symmetries. Given a state whose block MPS tensor is injective and satisfies Eq. (17), where $V(g)$ is a maximally non-commutative representation of a finite abelian group G , we would like to prove Eq. (20).

First, we prove Eq. (21). In general, if a state is invariant under the L -cycle symmetry in Eq. (16), then we have [63]

$$u(\phi^i(g)) \begin{array}{c} | \\ \hline \boxed{\mathcal{A}} \\ \hline \end{array} = W_i(g) \begin{array}{c} | \\ \hline \boxed{\mathcal{A}} \\ \hline \end{array} W_{i+1}(g)^\dagger, \quad (\text{B1})$$

for some unitaries $W_i(g)$ with $W_0(g) = W_L(g)$. This equation, and all others that follow in this section, hold for all $g \in G$. From Eq. (B1), we get

$$\begin{array}{c} u(g) \quad u(\phi(g)) \quad u(\phi^2(g)) \quad \dots \quad u(\phi^{L-1}(g)) \\ \begin{array}{c} | \\ \hline \boxed{\mathcal{A}} \\ \hline \end{array} \begin{array}{c} | \\ \hline \boxed{\mathcal{A}} \\ \hline \end{array} \begin{array}{c} | \\ \hline \boxed{\mathcal{A}} \\ \hline \end{array} \dots \begin{array}{c} | \\ \hline \boxed{\mathcal{A}} \\ \hline \end{array} \\ = \\ W_0(g) \begin{array}{c} | \\ \hline \boxed{\mathcal{A}} \\ \hline \end{array} \begin{array}{c} | \\ \hline \boxed{\mathcal{A}} \\ \hline \end{array} \begin{array}{c} | \\ \hline \boxed{\mathcal{A}} \\ \hline \end{array} \dots \begin{array}{c} | \\ \hline \boxed{\mathcal{A}} \\ \hline \end{array} W_0(g)^\dagger. \end{array} \quad (\text{B2})$$

If the block tensor is injective, the only way this equation and Eq. (17) can be compatible is if $W_0(g) \propto V(g)$. If we connect the relations in Eq. (B1) in a different order, we find

$$\begin{array}{c} u(\phi(g)) \quad u(\phi^2(g)) \quad u(\phi^3(g)) \quad \dots \quad u(g) \\ \begin{array}{c} | \\ \hline \boxed{\mathcal{A}} \\ \hline \end{array} \begin{array}{c} | \\ \hline \boxed{\mathcal{A}} \\ \hline \end{array} \begin{array}{c} | \\ \hline \boxed{\mathcal{A}} \\ \hline \end{array} \dots \begin{array}{c} | \\ \hline \boxed{\mathcal{A}} \\ \hline \end{array} \\ = \\ W_1(g) \begin{array}{c} | \\ \hline \boxed{\mathcal{A}} \\ \hline \end{array} \begin{array}{c} | \\ \hline \boxed{\mathcal{A}} \\ \hline \end{array} \begin{array}{c} | \\ \hline \boxed{\mathcal{A}} \\ \hline \end{array} \dots \begin{array}{c} | \\ \hline \boxed{\mathcal{A}} \\ \hline \end{array} W_1(g)^\dagger, \end{array} \quad (\text{B3})$$

where we have used the fact that $\phi^L(g) = g$. Now compare this to Eq. (17) with g replaced by $\phi(g)$. Again, by injectivity of the block tensor, we find that $W_1(g) \propto V(\phi(g))$. So, for some scalar $\lambda(g)$, we have

$$u(g) \begin{array}{c} | \\ \hline \boxed{\mathcal{A}} \\ \hline \end{array} = \lambda(g)V(g) \begin{array}{c} | \\ \hline \boxed{\mathcal{A}} \\ \hline \end{array} V(\phi(g))^\dagger. \quad (\text{B4})$$

Now, we would like to use Eq. (B4) to prove Eq. (20). This proof is similar to that of Theorem 1 in Ref. [31], adapted to L -cycle symmetries. First, we invoke maximal non-commutativity of the projective representation $V(g)$, which implies that it must have the form $\mathbb{I} \otimes \tilde{V}(g)$ in some basis, where $g \mapsto \tilde{V}(g)$ is irreducible. Then, if $u(g)$ is a linear representation, and $\tilde{V}(g)$ is irreducible projective representation with cocycle ω , Eq. (B4) tells us that $\lambda(g)\tilde{V}(\phi(g))$ must also have cocycle ω . By maximal non-commutativity of $\tilde{V}(g)$, we therefore have $\tilde{V}(\phi(g)) = \Phi^\dagger \tilde{V}(g) \Phi$ for some unitary Φ , and furthermore $g \mapsto \lambda(g)$ must be a 1D representation of G . Since $g \mapsto \lambda(g)$ is a representation, we can find Λ such that $\overline{\lambda(g)}\tilde{V}(g) = \Lambda^\dagger \tilde{V}(g) \Lambda$ [31]. Now we rewrite Eq. (B4) as

$$u(g) \begin{array}{c} | \\ \hline \boxed{\mathcal{A}} \\ \hline \end{array} = \mathbb{1} \otimes \tilde{V}(g) \begin{array}{c} | \\ \hline \boxed{\mathcal{A}} \\ \hline \end{array} \mathbb{1} \otimes \Phi^\dagger \Lambda^\dagger \tilde{V}(g)^\dagger \Lambda \Phi. \quad (\text{B5})$$

If we multiply each side by $\mathbb{I} \otimes \Phi^\dagger \Lambda^\dagger$ on the right, then we get a relation for the composite tensor $\mathcal{A}^\dagger(\mathbb{I} \otimes \Phi^\dagger \Lambda^\dagger)$. With this relation, we can continue as in Theorem 1 of Ref. [31] to obtain

$$\mathcal{A}^\dagger(\mathbb{I} \otimes \Phi^\dagger \Lambda^\dagger) = B^i \otimes C^i, \quad (\text{B6})$$

and

$$\mathcal{A}^i = B^i \otimes (C^i \Lambda \Phi). \quad (\text{B7})$$

This expression holds only with respect to the basis of physical spins $\{|i\rangle\}$ that diagonalizes $u(g)$, such that $u(g)|i\rangle = \chi_i(g)|i\rangle$ where $\chi_i(g)$ are 1D representations of G . We then have $C^i = \tilde{V}(g_i)$ where g_i are defined uniquely by the relation $\chi_i(g)\tilde{V}(g) = \tilde{V}(g_i)^\dagger \tilde{V}(g) \tilde{V}(g_i)$. B^i are unconstrained tensors and can vary throughout the SPT phase. Since λ is not uniformly defined throughout the SPT phase, Λ can also vary throughout the phase.

We would like to rewrite Eq. (B7) in such a way that we separate the parts which are universal throughout the phase, namely Φ and C^i , from the rest. We can accomplish this in the following way. On each block of L sites, we push the matrix Λ through the tensors to the end of the block,

$$\begin{aligned} B^{i_1} \dots B^{i_L} \otimes C^{i_1} \Lambda \Phi C^{i_2} \Lambda \Phi \dots C^{i_L} \Lambda \Phi = \\ B_{[1]}^{i_1} \dots B_{[L]}^{i_L} \otimes C^{i_1} \Phi \dots C^{i_L} \Phi \Lambda_*. \end{aligned} \quad (\text{B8})$$

Λ commutes with all $\tilde{V}(g_i)$ up to a phase. So when Λ passes through the tensor \mathcal{A}^i , it leaves behind a phase, which is absorbed into the tensor B^i . The tensors $B_{[j]}^i$ are the original tensors B^i along with these phases, which are in general not translationally invariant within a block (We do, however, have $B_{[j]}^i = B_{[j+L]}^i$). The matrix $\Lambda_* := \Lambda \Phi^{L-1} \Lambda \Phi^{L-1} \dots \Phi^\dagger \Lambda \Phi$ is a scalar matrix and can thus be removed from the above expression. To see this, note that Eq. (17) says that $\lambda(g)$ must satisfy the constraint

$$\lambda_*(g) := \lambda(g)\lambda(\phi(g)) \dots \lambda(\phi^{L-1}(g)) = 1. \quad (\text{B9})$$

By definition, we have $\overline{\lambda_*(g)}\tilde{V}(g) = \Lambda_*^\dagger \tilde{V}(g) \Lambda_*$. Since $\lambda_*(g) = 1$, we have $\Lambda_* \propto \mathbb{I}$ by Schur's lemma. The proportionality constant can be absorbed into one of the tensors $B_{[j]}^i$ and Λ_* can be removed from Eq. (B8). Hence, we can represent our state by an MPS of the form

$$A_{[j]}^i = B_{[j]}^i \otimes (C^i \Phi), \quad (\text{B10})$$

as desired. \square

C. Period of fractal CQCA

Here, we look at the period of fractal CQCA on rings of circumference N . This is in general a difficult problem to solve, and the period L could grow exponentially with N (see Table 5 for an example). Nevertheless, we prove that, for certain values of N , the period can be shown to have a linear

N	L	N	L	N	L
2	3	18	84	34	510
4	6	20	60	36	168
6	12	22	186	38	1026
8	12	24	48	40	120
10	30	26	126	42	2340
12	24	28	36	44	372
14	18	30	1020	46	12282
16	24	32	48	48	96

Figure 5. The period L as a function of the circumference N for the fractal QCA T_f in Eq. (13). For $N = 2^k$, the relationship is linear. In general, L appears to grow with an exponential envelope.

relation in general. Specifically, we prove that, for a fractal QCA T on a ring of circumference $N = 2^k$, the period is either $L = N = 2^k$ or $L = \frac{3}{2}N = 2^k + 2^{k-1}$. Throughout this proof, we will be taking powers of polynomials like $\sum_k c_k u^k$. Since we working over the field \mathbb{Z}_2 , we can write $(\sum_k c_k u^k)^{2^n} = \sum_k c_k (u^k)^{2^n}$, i.e. all cross terms cancel out. This simplifies the following calculations significantly.

Let

$$\gamma := \text{Tr}(t) = \beta + \sum_i \alpha^i (u^i + u^{-i}),$$

for $\alpha_i, \beta \in \{0, 1\}$. With the periodic boundary conditions, we identify $u^{-2^{k-1}}$ and $u^{2^{k-1}}$. Then we have

$$\gamma^{2^{k-1}} = \beta + \sum_i \alpha^i ((u^{2^{k-1}})^i + (u^{-2^{k-1}})^i) = \beta.$$

The proof now splits into two cases:

Case 1: $\beta = 0$. From Eq. (6), we have

$$t^{2^k} = (t^2)^{2^{k-1}} = (\gamma t + \mathbb{I})^{2^{k-1}} = \gamma^{2^{k-1}} t^{2^{k-1}} + \mathbb{I},$$

where cross terms again cancel out. Since $\gamma^{2^{k-1}} = \beta = 0$, we have $t^{2^k} = \mathbb{I}$, showing $L = 2^k = N$. \square

Case 2: $\beta = 1$. We need a formula for $t^{2^k + 2^{k-1}}$. The result, which we will prove by induction, is

$$t^{2^k + 2^{k-1}} = (1 + \gamma^{2^k}) \gamma^{2^{k-1} - 1} t + \left[(1 + \gamma^{2^k}) p_k(\gamma) + \gamma^{2^{k-1}} \right] \mathbb{I}. \quad (\text{C1})$$

Therein, $\gamma = \text{Tr}(t)$, and $p_k(\gamma)$ is some polynomial in γ . The expression is simple to confirm for $k = 1$ using Eq. (6), where $p_1(\gamma) = 0$. Now assume it is true for k . Then we have

$$t^{2^{k+1} + 2^k} = (t^{2^k + 2^{k-1}})^2 = (1 + \gamma^{2^{k+1}}) \gamma^{2^k - 2} t^2 + \left[(1 + \gamma^{2^k}) p_k(\gamma) + \gamma^{2^{k-1}} \right]^2 \mathbb{I}. \quad (\text{C2})$$

Now, we apply Eq. (6) to find

$$t^{2^{k+1} + 2^k} = (1 + \gamma^{2^{k+1}}) \gamma^{2^k - 1} t + \left[(1 + \gamma^{2^{k+1}}) p_{k+1}(\gamma) + \gamma^{2^k} \right] \mathbb{I}, \quad (\text{C3})$$

which is the desired expression where $p_{k+1}(\gamma) = p_k^2(\gamma) + \gamma^{2^k - 2}$. So the formula holds for all k . Now, since $\gamma^{2^{k-1}} = \beta = 1$, we get $t^{2^k + 2^{k-1}} = \mathbb{I}$, so $L = 2^k + 2^{k-1} = \frac{3}{2}N$. \square